

available at www.sciencedirect.comjournal homepage: www.elsevier.com/locate/carbon

Direct synthesis of carbon nanotubes decorated with size-controllable Fe nanoparticles encapsulated by graphitic layers

Qingfeng Liu, Wencai Ren, Zhi-Gang Chen, Bilu Liu, Bing Yu, Feng Li, Hongtao Cong, Hui-Ming Cheng*

Shenyang National Laboratory for Materials Science, Institute of Metal Research, Chinese Academy of Sciences, Shenyang 110016, PR China

ARTICLE INFO

Article history:

Received 20 February 2008

Accepted 2 June 2008

Available online 12 June 2008

ABSTRACT

A simple method has been developed for direct synthesis of magnetic multi-walled carbon nanotubes (MWCNTs) homogeneously decorated with size-controllable Fe nanoparticles (Fe-NPs) encapsulated by graphitic layers on the MWCNT surface by pyrolysis of ferrocene. These composites have similar C/Fe atomic ratio of ~ 10 and exhibit sufficiently high saturation magnetization for magnetic separation in a liquid phase. Moreover, with 0, ~ 1 , ~ 2 wt% sulfur as growth promoter, the size of Fe-NPs can be controlled with an average diameter of ~ 5 , ~ 22 and ~ 42 nm, respectively. When compared to time-consuming wet-chemical methods, the simplicity of this method should allow easy large-scale production of these magnetically functionalized MWCNTs, which can be used as catalyst supports with high stability for effective magnetic separation in liquid-phase reactions, especially under acid/basic conditions.

© 2008 Elsevier Ltd. All rights reserved.

1. Introduction

It is known that a smaller catalyst particle means a higher activity and experiences no significant attrition (no reduction in particle size) in liquid-phase reactions [1]. Consequently, both the activity and the stability of solid catalysts suspended in a liquid phase can benefit greatly from the utilization of catalyst nanoparticles (NPs). Moreover, catalyst supports are usually used in catalytic processes in order to achieve high dispersion, maximum utilization, as well as to avoid catalyst agglomeration and consequently realize a high catalysis performance [2]. Considering that with solid catalysts suspended within liquids the transport within the liquid to the surface of catalyst supports is proportional to $1/D^2$ (D , the diameter of catalyst supports) [3], it is attractive to utilize small catalyst supports to avoid transport limitations, and thus to raise the rate of the liquid-phase catalytic reactions. A very important issue in a liquid catalytic process is that the separation of these supports with nano-sized catalysts from the reaction

products is almost impossible by conventional means such as centrifugation and filtration, since they can easily lead to the blocking of filters and valves [4,5]. The efficient separation of suspended magnetic supports of nanocatalysts from the liquid products by using an external magnetic field offers a solution to this problem. For example, small magnetic supports are used to host enzymes or other biological materials that can only function under narrow or restricted reaction conditions [6–9]. However, most supports are chemically unstable under the conditions such as acidic, basic, corrosive, oxidizing, reducing environments or elevated temperatures, which are commonly encountered in catalytic fine-chemical synthesis. Recently, carbon nanotubes (CNTs) as nano-carbon catalyst support have drawn a growing interest due to their specific characteristics such as large surface area to volume ratio, good adsorption, unique structure, and high thermal and chemical stability [10–12]. As a result, CNTs decorated with magnetic NPs may provide an ideal candidate as catalyst support for effective magnetic separation in a liquid phase.

* Corresponding author: Fax: +86 24 2390 3126.

E-mail address: cheng@imr.ac.cn (H.-M. Cheng).

0008-6223/\$ - see front matter © 2008 Elsevier Ltd. All rights reserved.

doi:10.1016/j.carbon.2008.06.021

Generally, owing to the chemically stable and highly hydrophobic nature of the CNT surface, wet decoration methods are commonly employed for the decoration of CNTs with magnetic NPs of elements or compounds [13–22]. By wet decoration routes, CNTs can be decorated with magnetic NPs of several to tens of nanometers, which easily give sufficiently high saturation magnetization for magnetic separation. However, such CNTs are not suitable for magnetic support of nanocatalysts in a liquid phase, because (i) the magnetic NPs are just attached to the CNT surface, and thus can be easily peeled off from the CNT surface during liquid-phase reactions, especially with violent stirring, and (ii) the magnetic NPs are fairly reactive not only with acids but also with complex agents, which are often encountered in liquid-phase catalytic reactions. Therefore, in order to further realize the application of CNTs in heterogeneous catalysis, two structural characteristics should be satisfied for magnetically functioned CNTs as catalyst support. Firstly, strong linkage between the magnetic NPs and the CNTs is required. Secondly, it is necessary to completely shield the inner magnetic core from external environments with ideal “safety spacer” such as graphitic shells that are chemically inert and impermeable to most chemicals, while the catalytically active part located on the CNT surface can perform its function with no interference from the core.

This paper reports a simple method for direct synthesis of multi-walled carbon nanotubes (MWCNTs) decorated with magnetic Fe nanoparticles (Fe-NPs) encapsulated with graphitic layers by pyrolysis of ferrocene in chemical vapor deposition (CVD) growth process. By changing the experimental conditions, the size of Fe-NPs can be controlled with an average diameter of ~ 5 , ~ 22 and ~ 42 nm. These MWCNT/Fe-NP composites exhibit sufficiently high saturation magnetization for magnetic separation in a liquid phase. Moreover, chemical linkage between the Fe-NPs and the MWCNTs is found to tightly fasten Fe-NPs on the MWCNT surface. As a result, the complete encapsulation of the magnetic core anchored onto the surface of MWCNTs allows direct handling of intrinsically sensitive magnetic materials (Fe and Fe_3C) in acid/basic solution or in air, and hence separation of these catalyst supports in an external magnetic field can be achieved.

2. Experimental

The synthesis was performed in a quartz tube reactor (i.d. 40 mm) inside an electrical furnace. In a typical experiment, ~ 2000 sccm Ar flow was used as a carrier gas through the quartz tube. When the temperature of the center of the furnace reached 1100°C , ~ 100 mg ferrocene/sulfur mixture ($S = 0\text{--}3$ wt%) was sublimated in the temperature range of $120\text{--}250^\circ\text{C}$, and then the MWCNT/Fe-NP composites (40–70 mg) grew downstream in the region of $700\text{--}1000^\circ\text{C}$. After the growth, the furnace was cooled naturally to room temperature under the protection of Ar.

The samples were characterized by using scanning electron microscope (SEM, LEO SUPRA35 at 15 kV), transmission electron microscope (TEM, JEOL2010 and TecnaiG2 F30 at 200 kV), thermogravimetric analyzer (NETZSCH STA 449C), X-ray diffractometer (XRD, CuK_α radiation), and superconducting quantum interference device (SQUID) magnetometer.

3. Results and discussion

Depending on the growth conditions with 0, ~ 1 , ~ 2 wt% sulfur as growth promoter, three kinds of MWCNT/Fe-NP composites are obtained and denoted as S_i , S_{ii} , and S_{iii} , respectively. Fig. 1 shows the typical SEM images of these samples that consist of abundant MWCNTs. The whole surface of these MWCNTs is homogeneously decorated with uniform Fe-NPs, whose size is well controlled by the content of sulfur in the starting mixture. EDX analysis reveals that all samples have a similar C/Fe atomic ratio of ~ 10 , proximate to the fixed C/Fe ratio of ferrocene molecule, i.e. $\text{Fe}(\text{C}_5\text{H}_5)_2$. This result indicates that carbon and iron atoms from pyrolysis of ferrocene can be effectively transformed into such nanostructured composites. Thermogravimetric analysis (TGA) in air indicates that these samples have similar oxidation resistance (Fig. 2). There is a slight weight increase at around 500°C , which can be ascribed to the oxidation of Fe-NPs. The MWCNTs themselves are oxidized in a narrow temperature range of $520\text{--}620^\circ\text{C}$, with the comparable residual metal oxide (44–46 wt %), which is in agreement with EDX analysis.

It is found that sulfur exerts an important influence on the size of Fe-NPs anchored on the MWCNT surface, because all other experimental parameters are unchangeable. Fig. 3a is the TEM image of S_i produced by pyrolysis of pure ferrocene. The diameter of the Fe-NPs on the MWCNT surface measured from TEM images is in the range of 4–21 nm, with a Gaussian mean diameter of ~ 9.7 nm (Fig. 3b). When a quantity of ~ 1 wt% sulfur is used as growth promoter in the starting mixture, smaller Fe-NPs are anchored on the MWCNT surface in a uniform way (Fig. 3c). Fig. 3d represents the corresponding diameter histogram of these Fe-NPs, revealing that the diameter distribution is in a narrow range of 2–14 nm, with a Gaussian mean diameter of ~ 5 nm. Interestingly, with ~ 2 wt % sulfur in the starting mixture, the Fe-NPs with larger diameters are anchored onto the MWCNT surface (Fig. 3e). The diameters of these Fe-NPs are also in a larger range of 25–65 nm, with a Gaussian mean diameter of ~ 41 nm (Fig. 3f). Considering the comparable C/Fe atomic ratio of ~ 10 for these MWCNT/Fe-NP composites, it is natural and comprehensible that the particle density on the MWCNT surface decreases with the increase of the size of Fe-NPs.

The formation mechanism of these MWCNT/Fe-NP composites can be well explained, based on the vapor–liquid–solid (VLS) model. At elevated temperatures, ferrocene molecules quickly decompose to Fe clusters, floating carbon and hydrogen atoms. Due to the dissolution of carbon and the small size, the melting point of Fe clusters is far below the melting point of the bulk metal [23]. This suggests that Fe clusters are in a liquid state during the decomposition and suddenly contract to form liquid Fe-NPs because of surface tension. As the reaction proceeds, some Fe-NPs gradually become larger and act as the nucleation seeds for the growth of MWNTs when the carbon concentration inside these catalyst particles exceeds supersaturation. Meanwhile, due to the high ratio of Fe/C concentration in the reaction system and the strong affinity between Fe and C, liquid Fe-NPs are superfluous and tend to deposit on the sidewalls of the newly-formed MWNTs. Addition of a small quantity of sulfur can effectively enhance the formation of the

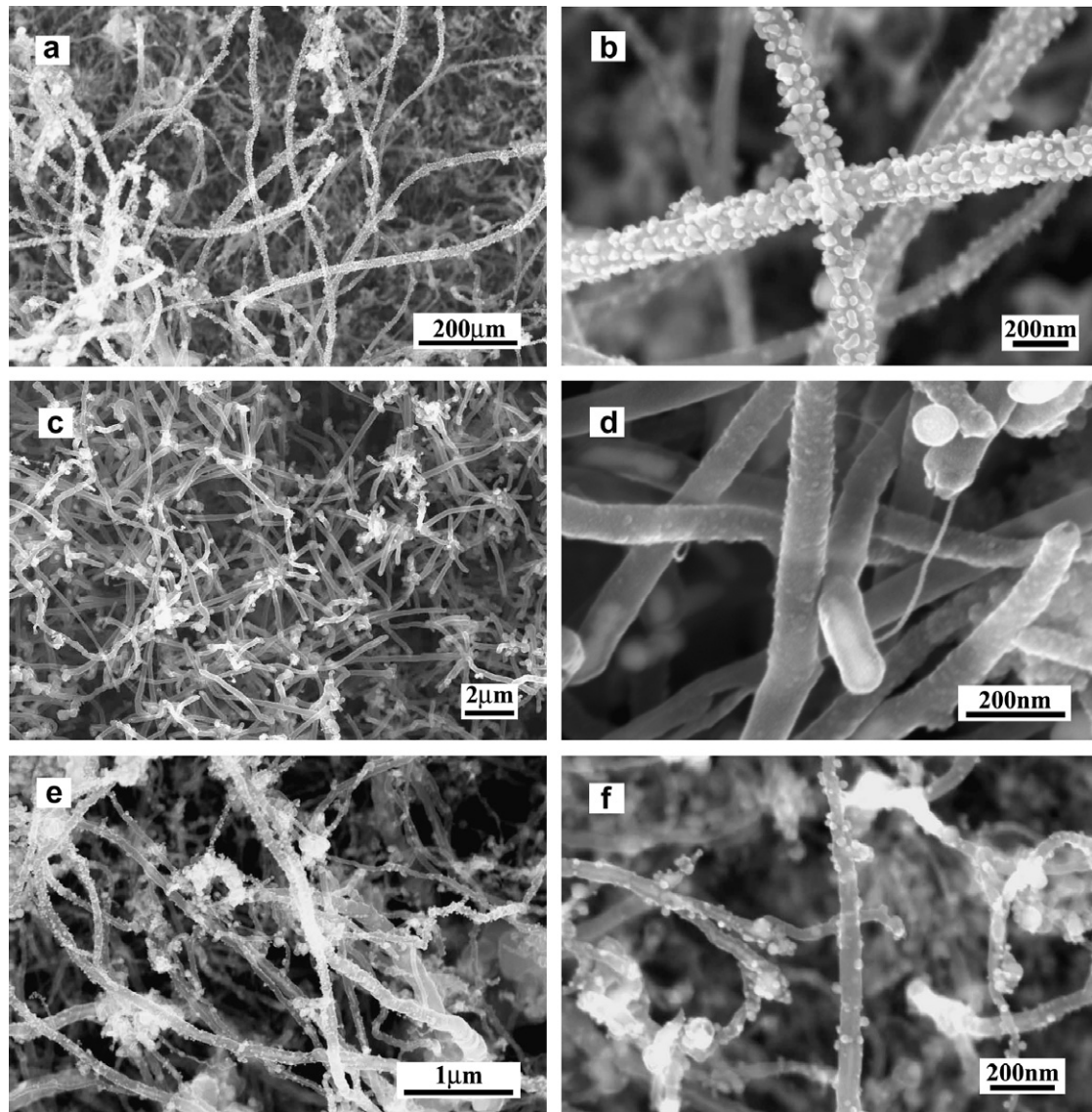


Fig. 1 – Typical SEM images of (a and b) S_i , (c and d) S_{ii} , and (e and f) S_{iii} .

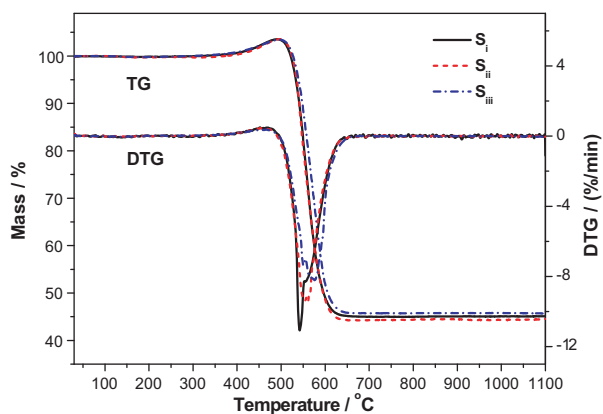


Fig. 2 – TGA curves of S_i , S_{ii} and S_{iii} in the airflow.

MWNT/Fe-NP composite, because S easily combines with C in the vapor phase at elevated temperatures, forms S-rich carbon clusters, and hence assists the graphitizing nanotubes

[24]. In addition, sulfur has a dramatic effect on the activity of Fe-NPs through surface reconstruction [25,26], and simultaneously increases the defects on the surface of the formed nanotubes [27]. This facilitates the decoration of Fe-NPs on the MWCNT surface, especially on the defects, which act as nucleation sites for the anchoring of Fe-NPs. Moreover, the local zones adsorbed with sulfur on the Fe-NP surface have a high adhesion energy toward graphite [27,28], which can strengthen strong linkage between Fe-NPs and the MWCNTs. However, a large quantity of S has increased the size of Fe-NPs in our experiments. The possible reason is that S has a high affinity to metal atoms due to the strong bonding between them, which is in favor to the aggregation of Fe clusters and forms larger Fe-NPs [26].

As mentioned above, although a variety of magnetic NPs ranging from several to tens of nanometers in size can be attached on the MWCNT surface by wet chemical methods [13–22], it is not easy for wet strategies to obtain such uniform decoration of MWCNTs with tiny Fe-NPs such as S_{ii} obtained

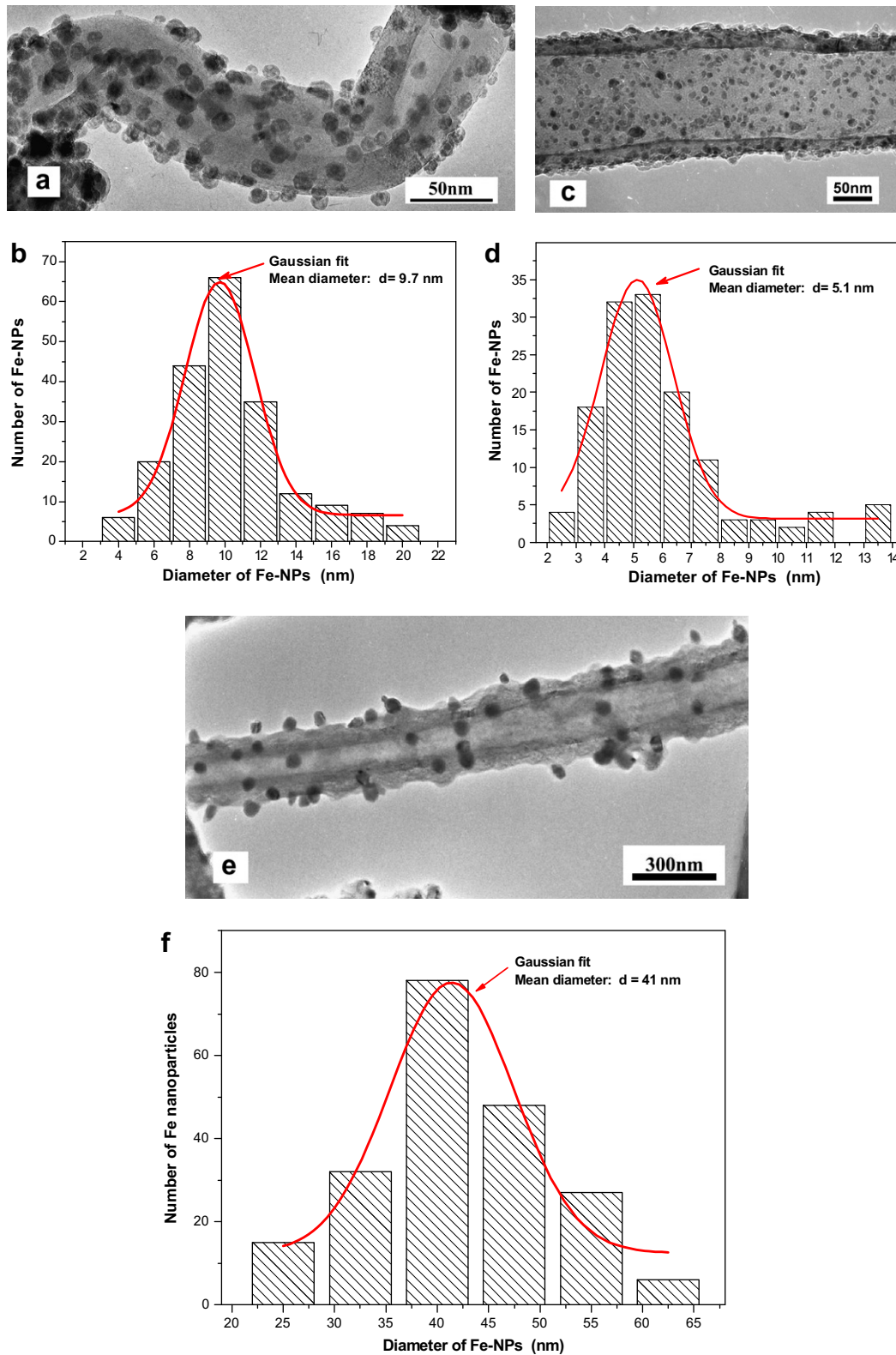


Fig. 3 – Typical TEM images and diameter distributions of the Fe-NPs of (a and b) S_{I} , (c and d) S_{II} , and (e and f) S_{III} .

by our method. Fig. 4a is high-resolution TEM (HRTEM) image of S_{III} , further revealing the MWCNTs decorated with ~ 5 nm Fe-NPs, which are encapsulated with several graphitic layers. The Fe-NPs are crystalline and have a lattice fringe spacing of 0.20 nm, related to the (110) plane of the α -Fe crystal

(JCPDS06-0696); the spacing of the lattice fringes of MWCNTs is ~ 0.34 nm, which is close to that of the graphite (002) planes. It can be seen that the highly ordered lattice fringes of single-crystal metal are vanished in the area adjacent to the Fe-MWCNT interface, which directly confirms strong

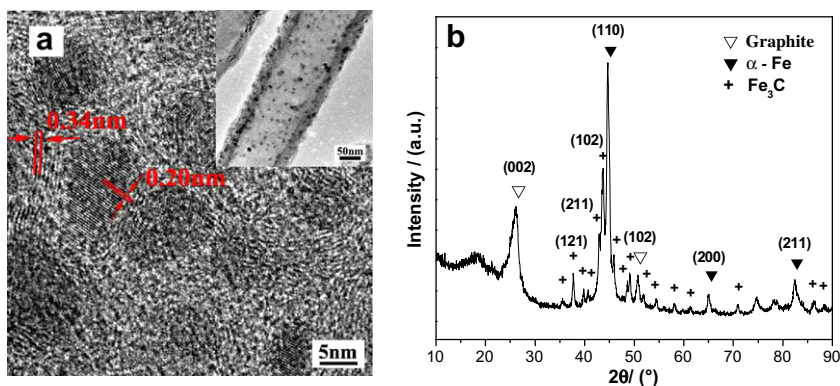


Fig. 4 – (a) HRTEM image (taken from a section in the inset) and (b) XRD pattern of S_{ii} .

chemical linkage between Fe-NPs and the MWCNTs [29]. Obviously, the strong interaction between the Fe-NPs and the MWCNT surface will be advantageous when this composite is used as magnetic supports for heterogeneous nanocatalysts in liquid-phase reactions, especially with violent stirring. Fig. 4b shows the XRD pattern for S_{ii} . The peaks at 44.7° , 65.0° and 82.3° can be identified as the (110), (200) and (211) planes of crystalline body-centered cubic (bcc) α -iron, respectively. A large fraction of orthorhombic cementite Fe_3C phase is also seen in the XRD pattern. The peak at about 26.2° is assigned to the (002) plane of hexagonal graphitic

structure of MWCNTs. This peak is symmetric and narrow, indicating a relatively high crystalline dimension.

To evaluate the magnetic properties of S_{ii} , SQUID magnetometer was used for magnetic characterization of this sample at room temperature, as shown in Fig. 5a. The smooth S-shaped curve has a saturation magnetization (M_s) of ~ 60 emu/g. Considering the small size of Fe-NPs decorated on the MWCNT surface, it is expected that a reduction of M_s occurs, compared to bulk iron ($M_s = 222$ emu/g) [30]. Moreover, the small coercivity of S_{ii} should not result in the clustering of this composite due to the mutual magnetic attraction, which

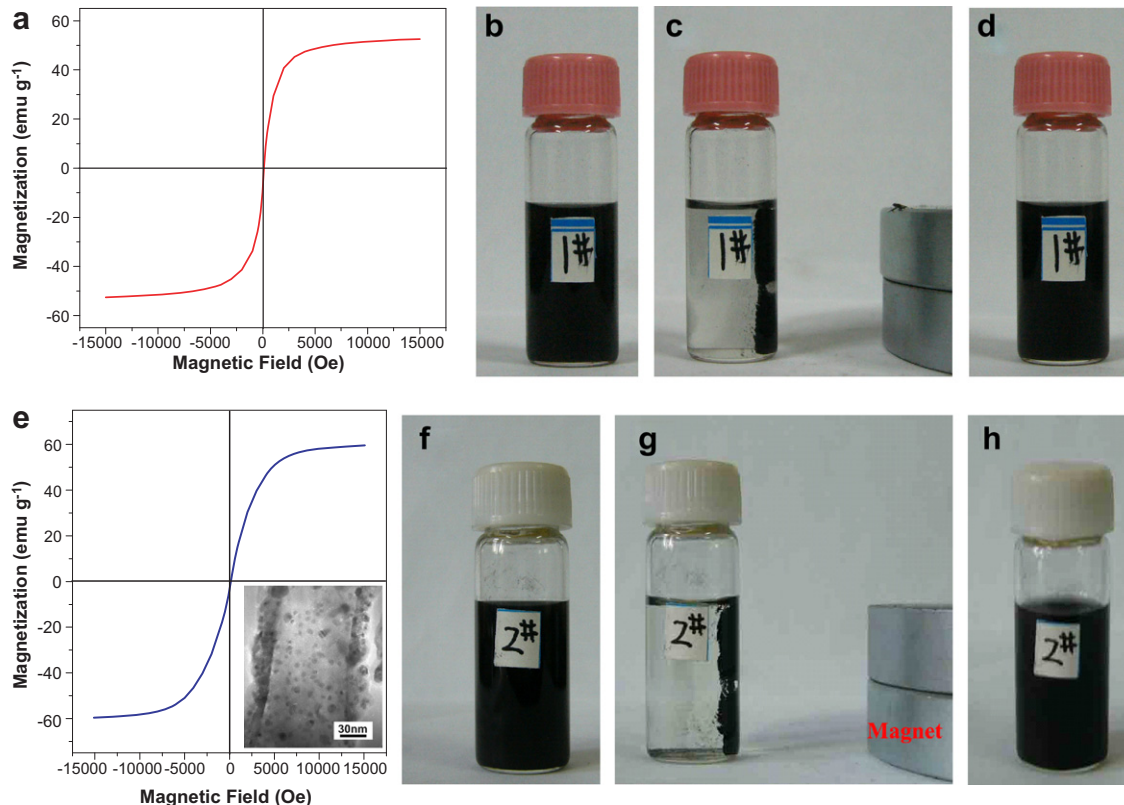


Fig. 5 – (a) Magnetization curve measured at room temperature for S_{ii} . (b) S_{ii} dispersion in ethanol. (c) Response of S_{ii} to a magnet. (d) Redisperison of S_{ii} in ethanol. (e) Magnetization curve measured at room temperature for the HNO_3 -treated S_{ii} (inset, showing the TEM image of HNO_3 -treated S_{ii}). (f) The HNO_3 -treated S_{ii} dispersion in ethanol. (g) Response of the HNO_3 -treated S_{ii} to a magnet. (h) The HNO_3 -treated S_{ii} redisperison in ethanol.

is proved by the following simple experiment to demonstrate the potential of such composite as reusable catalyst support for magnetic separation in a liquid phase. Fig. 5b shows S_{ii} well-dispersed in ethanol. The magnetic response of S_{ii} is easily and quickly visualized when it is moved towards a small magnet, and the clear solution after the magnetic separation is shown in Fig. 5c. After the magnet was removed, only gentle shaking could make the composite easily redisperse (Fig. 5d). Clearly, the magnetostatic attraction from the remanent magnetic moment (the magnetic moment in the absence of a magnetic field) is quite low, and does not lead to the clustering of MWCNTs. It is attributed to that the magnetic interaction is effectively decreased by the relatively large mutual distance of the fastened Fe-NPs on the MWCNT surface by strong chemical linkage. Meanwhile, the graphitic shells of the Fe-NPs and the MWCNTs act as non-magnetic separation, which is also essential for the Fe-NPs to eliminate the dipolar interaction between the neighboring ones [31].

As mentioned above, an important advancement is that the inner magnetic core is completely shielded from external environments with impermeable graphitic layers, consequently ensuring long-term stability of the ferromagnetic core. To validate this protection of graphitic layers on the encapsulated Fe-NPs, S_{ii} was treated in concentrated HNO_3 (~65 wt%) for 30 h. Magnetic characterization of the HNO_3 -treated S_{ii} also shows S-shaped magnetization curve with a comparable small coercivity (Fig. 5e). It is observed that the Fe-NPs are still anchored on the MWCNT surface after the HNO_3 -treatment (the inset of Fig. 5e). In addition, a similar magnetic response of the resulting sample in solution is observed, as shown in Fig. 5f–h. Moreover, the HNO_3 -treated composite shows a good dispersion in organic solvent or distilled water, because some functional groups such as $-NO_3$ and $-C=O$ were attached to the surface of MWCNTs during the harsh acidic treatment. The high stability of this composite is significantly advantageous when it is used as magnetic support of heterogeneous nanocatalysts in liquid-phase reactions, especially under severe conditions such as acidic, corrosive or oxidizing environments, etc. For example, sulphided Co–Mo–K catalysts supported by Co-decorated MWCNTs have demonstrated to display higher catalytic activity and selectivity for higher alcohol synthesis from syngas, when compared to the reference catalyst supported by the simple MWCNTs or conventional activated carbon [32].

4. Conclusions

We have developed a simple method for synthesis of MWCNTs decorated with size-controllable Fe-NPs from pyrolysis of ferrocene by controlling sulfur content in the starting mixture. The Fe-NPs are encapsulated with graphitic layers and tightly anchored on the MWCNT surface by chemical linkages, and thus have high stability under acidic, corrosive or oxidizing environments. The structural properties of these composites make them not only exhibit sufficiently strong magnetic response for ease of separation, but also effectively prevent the clustering of MWCNTs. Furthermore, by pyrolysis of metallocenes such as ferrocene, nickelocene, cobaltocene or their mixtures, this technology is also expected to easily

prepare Fe/Ni/Co NPs decorating CNTs with tunable magnetic properties, which can find various applications in nanoelectronic devices, magnetic resonance imaging, and magnetic data storage.

Acknowledgements

The work was supported by Ministry of Science and Technology of China (No. 2006CB932701), National Science Foundation of China (No. 90606008), and Chinese Academy of Sciences (No. KJCX2-YW-M01).

REFERENCES

- [1] Tsang SC, Caps V, Paraskevas I, Chadwick D, Thompsett D. Magnetically separable, carbon-supported nanocatalysts for the manufacture of fine chemicals. *Angew Chem-Int Edit* 2004;43(42):5645–9.
- [2] Planeix JM, Coustel N, Coq B, Brotons V, Kumbhar PS, Dutartre R, et al. Application of carbon nanotubes as supports in heterogeneous catalysis. *J Am Chem Soc* 1994;116(17):7935–6.
- [3] Teunissen W, Bol AA, Geus JW. Magnetic catalyst bodies. *Catal Today* 1999;48(1–4):329–36.
- [4] Teunissen W, de Groot FMF, Geus J, Stephan O, Tence M, Colliex C. The structure of carbon encapsulated NiFe nanoparticles. *J Catal* 2001;204(1):169–74.
- [5] Lu AH, Schmidt W, Matoussevitch N, Bonnemann H, Spliethoff B, Tesche B, et al. Nanoengineering of a magnetically separable hydrogenation catalyst. *Angew Chem-Int Edit* 2004;43(33):4303–6.
- [6] Arica MY, Yavuz H, Patir S, Denizli A. Immobilization of glucoamylase onto spacer-arm attached magnetic poly(methylmethacrylate) microspheres: characterization and application to a continuous flow reactor. *J Mol Catal B-Enzym* 2000;11(2–3):127–38.
- [7] Gao X, Yu KMK, Tam KY, Tsang SC. Colloidal stable silica encapsulated nano-magnetic composite as a novel biocatalyst carrier. *Chem Commun* 2003;24:2998–9.
- [8] Reetz MT, Zonta A, Vijayakrishnan V, Schimossek K. Entrapment of lipases in hydrophobic magnetite-containing sol-gel materials: magnetic separation of heterogeneous biocatalysts. *J Mol Catal A-Chem* 1998;134(1–3):251–8.
- [9] Tang DP, Yuan R, Chai YQ, An HZ. Magnetic-core/porous-shell $CoFe_2O_4/SiO_2$ composite nanoparticles as immobilized affinity supports for clinical immunoassays. *Adv Funct Mater* 2007;17(6):976–82.
- [10] Serp P, Corrias M, Kalck P. Carbon nanotubes and nanofibers in catalysis. *Appl Catal A-Gen* 2003;253(2):337–58.
- [11] Liu QF, Ren WC, Li F, Cong HT, Cheng HM. Synthesis and high thermal stability of double-walled carbon nanotubes using nickel formate dihydrate as catalyst precursor. *J Phys Chem C* 2007;111(13):5006–13.
- [12] Ebbesen TW, Hiura H, Bisher ME, Treacy MMJ, ShreeveKeyer JL, Haushalter RC. Decoration of carbon nanotubes. *Adv Mater* 1996;8(2):155–7.
- [13] Unger E, Duesberg GS, Liebau M, Graham AP, Seidel R, Kreupl F, et al. Decoration of multi-walled carbon nanotubes with noble- and transition-metal clusters and formation of CNT–CNT networks. *Appl Phys A-Mater Sci Process* 2003;77(6):735–8.
- [14] Stoffelbach F, Aqil A, Jerome C, Jerome R, Detrembleur C. An easy and economically viable route for the decoration of carbon nanotubes by magnetite nanoparticles, and their

- orientation in a magnetic field. *Chem Commun* 2005;36:4532–3.
- [15] Jang JS, Yoon HS. Fabrication of magnetic carbon nanotubes using a metal-impregnated polymer precursor. *Adv Mater* 2003;15(24):2088–91.
- [16] Correa-Duarte MA, Grzelczak M, Salgueirino-Maceira V, Giersig M, Liz-Marzan LM, Farle M, et al. Alignment of carbon nanotubes under low magnetic fields through attachment of magnetic nanoparticles. *J Phys Chem B* 2005;109(41):19060–3.
- [17] Cao HQ, Zhu MF, Li YG. Decoration of carbon nanotubes with iron oxide. *J Solid State Chem* 2006;179(4):1208–13.
- [18] Wu HQ, Yuan PS, Xu HY, Xu DM, Geng BY, Wei XW. Controllable synthesis and magnetic properties of Fe–Co alloy nanoparticles attached on carbon nanotubes. *J Mater Sci* 2006;41(20):6889–94.
- [19] Wu HQ, Cao YJ, Yuan PS, Xu HY, Wei XW. Controlled synthesis, structure and magnetic properties of $\text{Fe}_{1-x}\text{Ni}_x$ alloy nanoparticles attached on carbon nanotubes. *Chem Phys Lett* 2005;406(1–3):148–53.
- [20] Georgakilas V, Tzitzios V, Gournis D, Petridis D. Attachment of magnetic nanoparticles on carbon nanotubes and their soluble derivatives. *Chem Mater* 2005;17(7):1613–7.
- [21] Cheng JP, Zhang XB, Ye Y. Synthesis of nickel nanoparticles and carbon encapsulated nickel nanoparticles supported on carbon nanotubes. *J Solid State Chem* 2006;179(1):91–5.
- [22] Jiang LQ, Gao L. Carbon nanotubes-magnetite nanocomposites from solvothermal processes: Formation, characterization, and enhanced electrical properties. *Chem Mat* 2003;15(14):2848–53.
- [23] Rummeli MH, Borowiak-Palen E, Gemming T, Pichler T, Knupfer M, Kalbac M, et al. Novel catalysts, room temperature, and the importance of oxygen for the synthesis of single-walled carbon nanotubes. *Nano Lett* 2005;5(7):1209–15.
- [24] Demoncy N, Stephan O, Brun N, Colliex C, Loiseau A, Pascard H. Filling carbon nanotubes with metals by the arc-discharge method: the key role of sulfur. *Eur Phys J B* 1998;4(2):147–57.
- [25] Rodriguez NM. A review of catalytically grown carbon nanofibers. *J Mater Res* 1993;8(12):3233–50.
- [26] Kim MS, Rodriguez NM, Baker RTK. The interplay between sulfur adsorption and carbon deposition on cobalt catalysts. *J Catal* 1993;143(2):449–63.
- [27] Ren WC, Li F, Bai S, Cheng HM. The effect of sulfur on the structure of carbon nanotubes produced by a floating catalyst method. *J Nanosci Nanotechnol* 2006;6(5):1339–45.
- [28] Dujardin E, Ebbesen TW, Hiura H, Tanigaki K. Capillarity and wetting of carbon nanotubes. *Science* 1994;265(5180):1850–2.
- [29] Golberg D, Mitome M, Muller C, Tang C, Leonhardt A, Bando Y. Atomic structures of iron-based single-crystalline nanowires crystallized inside multi-walled carbon nanotubes as revealed by analytical electron microscopy. *Acta Mater* 2006;54(9):2567–76.
- [30] Nikitenko SI, Kolytyn Y, Palchik O, Felner I, Xu XN, Gedanken A. Synthesis of highly magnetic, air-stable iron iron carbide nanocrystalline particles by using power ultrasound. *Angew Chem-Int Edit* 2001;40(23):4447–9.
- [31] Zhang XX, Wen GH, Huang SM, Dai LM, Gao RP, Wang ZL. Magnetic properties of Fe nanoparticles trapped at the tips of the aligned carbon nanotubes. *J Magn Magn Mater* 2001;231(1):L9–L12.
- [32] Ma XM, Lin GD, Zhang HB. Co-decorated carbon nanotube-supported Co–Mo–K sulfide catalyst for higher alcohol synthesis. *Catal Lett* 2006;111(3–4):141–51.